

A NUMERICAL STUDY OF THE STEADY STATE FREEZING OF WATER IN AN OPEN RECTANGULAR CAVITY

P.H. OOSTHUIZEN AND J.T. PAUL

Heat Transfer Laboratory, Department of Mechanical Engineering, Queen's University, Kingston, Ontario, K7L 3N6 Canada

ABSTRACT

A numerical study of the flow in and heat transfer across a vertical cavity containing pure water when the aspect ratio of the cavity is low, i.e. 1 or less, has been undertaken. One vertical wall of the cavity is kept at a temperature that is below the freezing point of water while the opposite wall is kept at a temperature that is above this freezing temperature. Ice therefore forms in part of the cavity, the conditions being such that there can be significant natural convection in the water. The upper surface of the cavity is open i.e. the water has a free surface, heat transfer from this surface being assumed negligible. The lower surface of the cavity is assumed to be adiabatic. Only the steady state has been considered here. It has been assumed that the flow is laminar and two-dimensional and that liquid and solid properties are constant except for the water density change with temperature which gives rise to the buoyancy forces. The governing equations have been written in dimensionless form and these equations have been solved using a finite element-based procedure in which the position of the solid-liquid interface is obtained using an iterative approach. Solutions have been obtained for modified Rayleigh numbers of between 10^3 and 10^8 for various degrees of under-cooling and for cavity aspect ratios of between 0.25 and 1. The density inversion that occurs with water has been shown to have a large effect on the steady state freezing of water in a cavity. The aspect ratio of the cavity has also been shown to have a significant influence on the results when the aspect ratio is less than 0.5.

KEY WORDS Solidification Natural convection Density inversion Heat transfer Numerical methods

NOMENCLATURE

A = Aspect ratio, H/W'	u = Dimensionless velocity component in x direction
a = Coefficient in density-temperature relation	u' = Velocity component in x' direction
c = Specific heat	v = Dimensionless velocity component in y direction
g = Gravitational acceleration	v' = Velocity component in y' direction
H' = Height of cavity	W' = Width of cavity
k = Thermal conductivity	x = Dimensionless x' co-ordinate
k_r = Ratio of solid to liquid thermal conductivities	x' = Horizontal co-ordinate position
Nu = Mean Nusselt number based on W'	y = Dimensionless y' co-ordinate
n = n'/W'	y' = Vertical co-ordinate position
n' = Co-ordinate measured normal to a surface	<i>Greek symbols</i>
Pr = Prandtl number	α = Thermal diffusivity
q = Mean heat transfer rate	Δ = Mean dimensionless liquid layer thickness
Ra = Modified Rayleigh number based on W'	ν = Kinematic viscosity
S = S/W'	ρ = Density
S' = Local distance from hot wall to ice/water interface	ρ_M = Maximum density
T = Dimensionless temperature	ψ = Dimensionless stream function
T' = Temperature	ψ' = Stream function
T'_C = Temperature of cold surface	ω = Dimensionless vorticity
T'_F = Solidification temperature	ω' = Vorticity
T'_H = Dimensionless temperature of hot wall	<i>Subscripts</i>
T'_H = Temperature of hot wall	l = Liquid
T'_M = Dimensionless temperature of maximum density	s = Solid
T'_M = Temperature of maximum density	

0961-5539/96

© 1996 MCB University Press Ltd

Received January 1995

Revised September 1995

INTRODUCTION

The present study is concerned with the flow in and heat transfer across a vertical rectangular cavity containing pure water. One of the vertical walls of the cavity is kept at a temperature that is below the freezing point of water, while the opposite wall is kept at a temperature that is above this freezing temperature. As a result, ice forms in part of the cavity, the conditions being such that there can be significant natural convection in the unfrozen water. The upper surface of the cavity is open, i.e. the water has a free surface. This upper surface has been assumed to remain flat and the heat transfer from it has been assumed to be negligible. The lower surface of the enclosure has been assumed to be adiabatic. The flow situation is thus as shown in *Figure 1*. Only the steady state has been considered here, i.e. the evolution of the flow with time from some prescribed initial state has not been considered. Attention has been restricted to cavities with relatively low aspect ratios, i.e. aspect ratios of 1 or less.

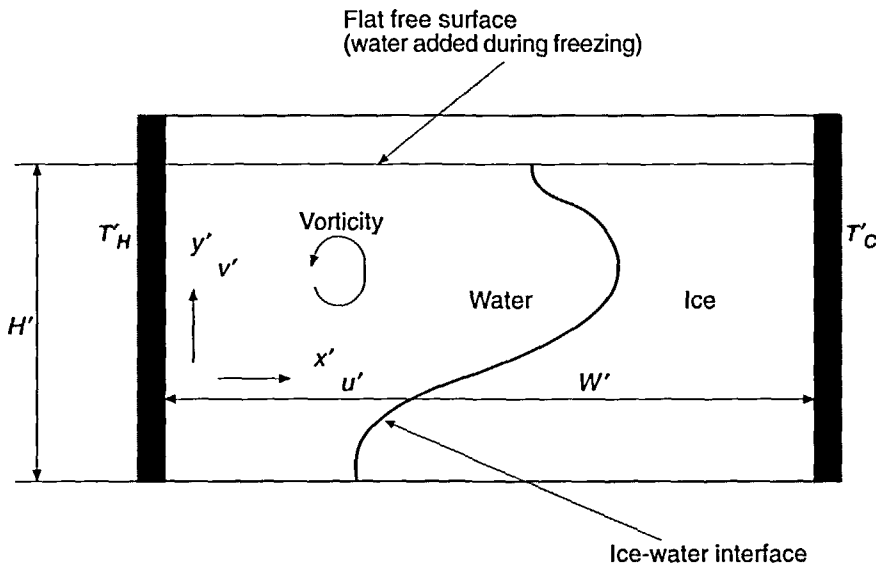


Figure 1 Flow configuration considered

There have been a number of previous studies of solidification and melting of liquids in a cavity. Almost all of these studies have, however, been concerned with the evolution of the flow with time and have not been concerned with a detailed study of the effects of the various governing parameters on the final steady state for the case where there is under-cooling. A review of much of this work is given by Yao and Prusa¹ and Fukusako and Yamada². Experimental and numerical studies of the particular case of the freezing of pure water in a rectangular enclosure are given by Braga and Viskanta³ and de Vahl Davis *et al.*⁴ respectively. These studies also provide reviews of past work on the subject. A numerical study of steady state freezing of water is described by Oosthuizen⁵ but results are, basically, only given for a square cavity. These studies all indicate that the density maximum that occurs near the freezing point with water may play an important role in the freezing of water in a rectangular enclosure. There have been a number of studies of natural convection in water in a cavity without freezing under such conditions that this density maximum is important, (e.g. see references 6 to 9, these papers also containing reviews of past work in this field). Several of these studies showed that quite sharp changes in the flow pattern in the cavity can occur as the result of relatively small changes in the wall temperatures when these temperatures are near the maximum density temperature.

Existing studies have not not given much consideration to the final steady state and have not considered a wide range of governing parameters. It was for this reason that the present study was undertaken.

GOVERNING EQUATIONS AND SOLUTION PROCEDURE

It has been assumed that the flow is steady, laminar and two-dimensional and that the liquid and solid properties are constant except for the water density change with temperature which gives rise to the buoyancy forces, this being treated by assuming a quadratic type relationship, i.e. by

$$(\rho_M - \rho)/\rho = a(T' - T'_M)^2 \tag{1}$$

the subscript *M* referring to conditions at the temperature of maximum density. This equation provides a good fit to the experimentally observed variation of the density of water with temperature between approximately 0°C and 10°C.

The solution for the water, in which the natural convection has been assumed to be important, has been obtained in terms of the stream function and vorticity defined, as usual, by:

$$u' = \frac{\partial \psi'}{\partial y'} , \quad v' = -\frac{\partial \psi'}{\partial x'}$$

$$\omega' = \frac{\partial v'}{\partial x'} - \frac{\partial u'}{\partial y'} . \tag{2}$$

The prime (') denotes a dimensional quantity. The co-ordinate system used is shown in *Figure 1*.

The following dimensionless variables have then been defined:

$$\psi = \psi' / \alpha , \quad \omega = \omega' W'^2 / \alpha$$

$$T = (T' - T'_F) / (T'_H - T'_C) \tag{3}$$

where $\alpha = k_l / \rho c$ is the thermal diffusivity of the water.

In terms of these dimensionless variables, the governing equations for the liquid flow are:

$$\frac{\partial^2 \psi}{\partial x^2} + \frac{\partial^2 \psi}{\partial y^2} = -\omega \tag{4}$$

$$\left(\frac{\partial^2 \omega}{\partial x^2} + \frac{\partial^2 \omega}{\partial y^2} \right) - \frac{1}{Pr} \left(\frac{\partial \psi}{\partial y} \frac{\partial \omega}{\partial x} - \frac{\partial \psi}{\partial x} \frac{\partial \omega}{\partial y} \right) = -2 Ra^* T \frac{\partial T}{\partial x} \tag{5}$$

$$\frac{\partial^2 T}{\partial x^2} + \frac{\partial^2 T}{\partial y^2} - \left(\frac{\partial y}{\partial y} \frac{\partial T}{\partial x} - \frac{\partial y}{\partial x} \frac{\partial T}{\partial y} \right) = 0 \tag{6}$$

where *Ra* * is the modified Rayleigh number defined by:

$$Ra^* = a g W'^3 (T_{H'} - T_{C'})^2 / \nu \alpha . \tag{7}$$

The equation governing the temperature distribution in the solid phase, i.e. the ice, is:

$$\frac{\partial^2 T}{\partial x^2} + \frac{\partial^2 T}{\partial y^2} = 0. \tag{8}$$

The boundary conditions on the solution are:

On all walls:

$$\psi = 0, \frac{\partial \psi}{\partial n} = 0$$

At $x = 0$:

$$T = T_H$$

At $x = 1$:

$$T = T_C (= T_H - 1)$$

On the bottom surface:

$$\frac{\partial T}{\partial y} = 0$$

where n is the co-ordinate measured normal to the surface considered. On the top surface, which is assumed to remain flat:

$$\psi = 0, \quad \omega = 0, \quad \frac{\partial T}{\partial y} = 0$$

On the interface between the water and ice, the following conditions apply:

$$\psi = 0, \quad \frac{\partial \psi}{\partial n} = 0$$

$$\left. \frac{\partial T}{\partial n} \right|_l = \left. \frac{\partial T}{\partial n} \right|_s \left(\frac{k_s}{k_l} \right)$$

where the subscripts l and s refer to conditions on the liquid and solid sides of the interface respectively. The condition on temperature at the interface has been obtained by noting that only the steady state is being considered here.

The above dimensionless equations, subject to the boundary conditions, have been solved using a finite element procedure. The solution is iterative in nature. The position of the solid-liquid interface is first guessed and the element distributions in the solid and liquid regions are selected, nodal points being selected to lie along solid-liquid interface. The solution is then started and, as it progresses, the interface position is locally modified according to the difference between the calculated rates of heat transfer at the interface on the solid and liquid sides, the element shapes being adaptively modified to follow the changing interface shape. The solution is continued until a converged solution is obtained.

Beside the streamline patterns in the cavity, the main results that will be presented here are the mean Nusselt number, Nu , based on the overall temperature difference and on the full width of the enclosure and the dimensionless mean liquid layer thickness Δ . These are defined by:

$$Nu = \frac{qW'}{k_l(T_H' - T_C')} \quad (9)$$

and

$$\Delta = \frac{l}{A} \int_0^A S dy. \quad (10)$$

The grid independence of the results was established by carrying out calculations for the same conditions for different numbers and distributions of elements.

RESULTS

The solution has the following parameters:

- The modified Rayleigh number, Ra^* ;
- the Prandtl number, Pr ;

- the aspect ratio of the rectangular cavity, A ;
- the ratio of the thermal conductivity of the frozen material to that of the unfrozen material, k_f ;
- the dimensionless temperature of the hot wall, T_H ;
- the dimensionless temperature at which the maximum density occurs, T_M .

Attention has here been restricted to a Prandtl number of 11 and a conductivity ratio, k_f , of 4. Solutions have been obtained for modified Rayleigh numbers of between 10^3 and 10^8 for cavity aspect ratios of between 0.25 and 1 for various degrees of under-cooling i.e. for various values of T_H since $T_C = 1 - T_H$. The value of T_M basically will be determined by the difference between the hot and cold wall temperatures because $(T'_M - T'_F)$ is approximately 4°C for water. Results will only be presented here for T_M equal 0.4, these results being typical of those obtained at all values of T_M . This value of T_M corresponds, physically, to a $(T'_H - T'_C)$ value of 10°C . Physically, then, the different values of the modified Rayleigh number considered here will correspond to different sizes of cavity.

The effect of aspect ratio and modified Rayleigh number on the streamline pattern and the shape of the ice-water interface will first be considered. *Figures 2 and 3* and *Figures 4 and 5* show typical streamline patterns and ice-water interface shapes for Ra^* values of 10^6 and 10^7 for cavity aspect ratios of 1 and 0.5 for various values of T_H while *Figure 6* show typical patterns and interface shapes for a cavity with an aspect ratio of 0.25 for a Ra^* value of 10^7 . It will be recalled that the present results are for T_M equals 0.4. When T_H is less than this value the flow basically consists of a single vortex which involves flow down the hot wall and up the interface. When T_H is increased above T_M , a second vortex associated with flow up the hot wall develops. The strength of this vortex then grows rapidly with increasing T_H while the strength of the original vortex decreases. It will be seen that the value of T_H at which the second vortex starts to become important decreases with increasing Ra^* . It will also be seen that with a cavity aspect ratio of 1, the clockwise-rotating vortex tends to be swept into the upper portion of the cavity as T_H is increased leading to a relative complex interface shape whereas at a cavity aspect ratio of 0.25, the two vortices remain next to each other. de Vahl Davis *et al.*⁴ presented two sets of results, in which the density maximum was taken into account, for the freezing of water in an enclosure. These results were for an enclosure with an aspect ratio of 1 and, although the values of the parameters used were not exactly the same as those used here, their solutions for long times (theirs was a transient solution) are very similar to those obtained here for the same dimensionless hot wall temperatures.

The changes in flow pattern with increasing T_H are further illustrated by the results given in *Figure 7*. This shows the variations of the maximum and minimum values of the dimensionless stream function with dimensionless hot wall temperature for various aspect ratios for $Ra^* = 10^7$. Positive values of the stream function are associated with a downward flow along the hot wall and an upward flow along the interface (a counterclockwise rotating vortex) while negative values are associated with a flow up the hot wall and down ice-water interface (a clockwise rotating vortex). It will again be seen from this figure that there is essentially no motion in the cavity at values of T_H below about 0.2. It will also be seen that, at low wall temperatures, the flow is entirely down the hot wall and up the cold wall but that when the hot wall temperature increases above the maximum density temperature, this motion starts to decrease in intensity and there is relatively rapid rise in the motion associated with flow up the hot wall and down the interface at the higher cavity aspect ratios considered.

At the lowest cavity aspect ratio considered, however, both vortices remain relatively weak and the strength of the clockwise rotating vortex grows relatively slowly with increasing dimensionless hot wall temperature.

The mean heat transfer rate across the enclosure will be considered next. *Figures 8 and 9* show the variations of mean Nusselt number with dimensionless hot wall temperature for various values of the modified Rayleigh number for cavities with aspect ratios of 1 and 0.5 respectively. It will

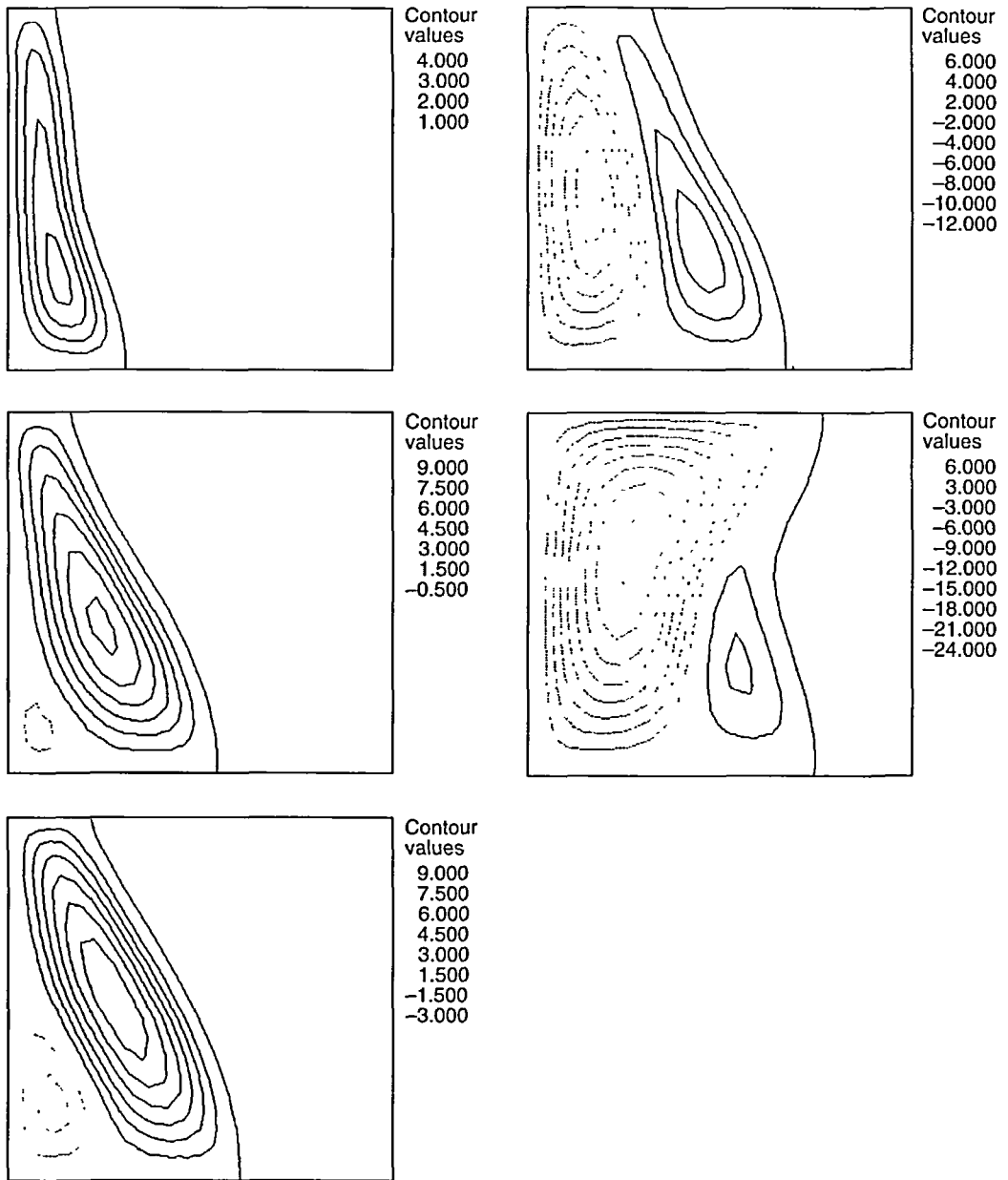


Figure 2 Streamline patterns in cavity with an aspect ratio of 1 for a modified Rayleigh Number of 10^6 for dimensionless hot wall temperatures of, from the top, 0.5, 0.6, 0.65, (left) 0.75 and 0.8 (right)

be seen from these figures that at low values of the dimensionless hot wall temperature, the Nusselt number is equal to the pure conduction value, this being given:

$$Nu = T_H + k_r(1 - T_H) \quad (11)$$

the conductivity ratio, k_r , it will be recalled, being taken as 4. As the dimensionless hot wall temperature increases, a point is reached at which the convective motion starts to become strong

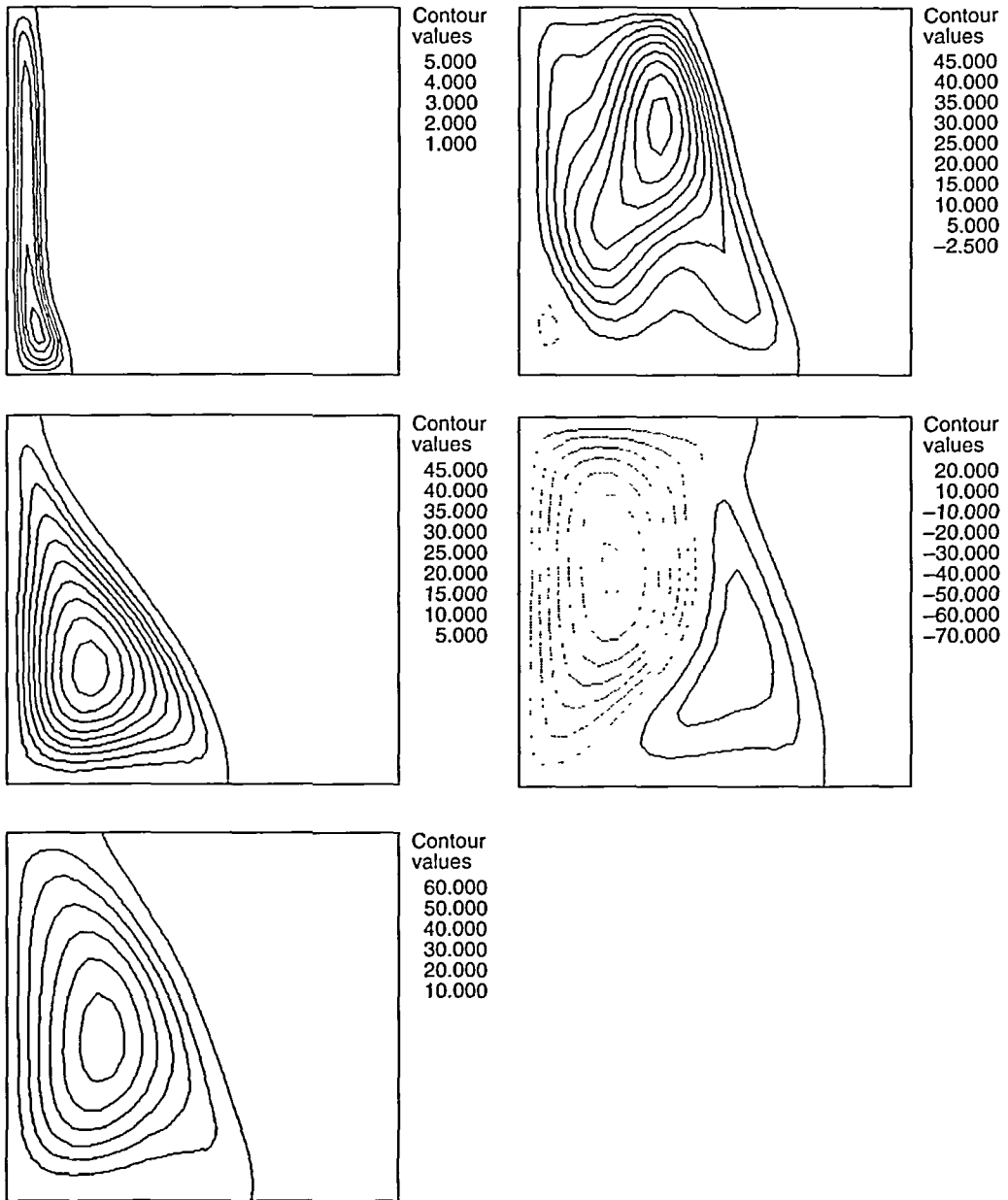


Figure 3 Streamline patterns in cavity with an aspect ratio of 1 for a modified Rayleigh Number of 10^7 for dimensionless hot wall temperatures of, from the top, 0.3, 0.4, 0.45, (left) 0.55 and 0.7, (right)

enough to influence the heat transfer rate, and the Nusselt number starts to rise above the pure conduction value. At the higher modified Rayleigh numbers, this occurs at hot wall temperatures that are well below the maximum density temperature. Under these circumstances, then, the flow is predominantly down the hot wall and up the cold wall because of the density inversion. When the hot wall temperature rises above the maximum density temperature an opposite flow starts to develop, as discussed before, which tends to first decrease the heat transfer rate. However, with

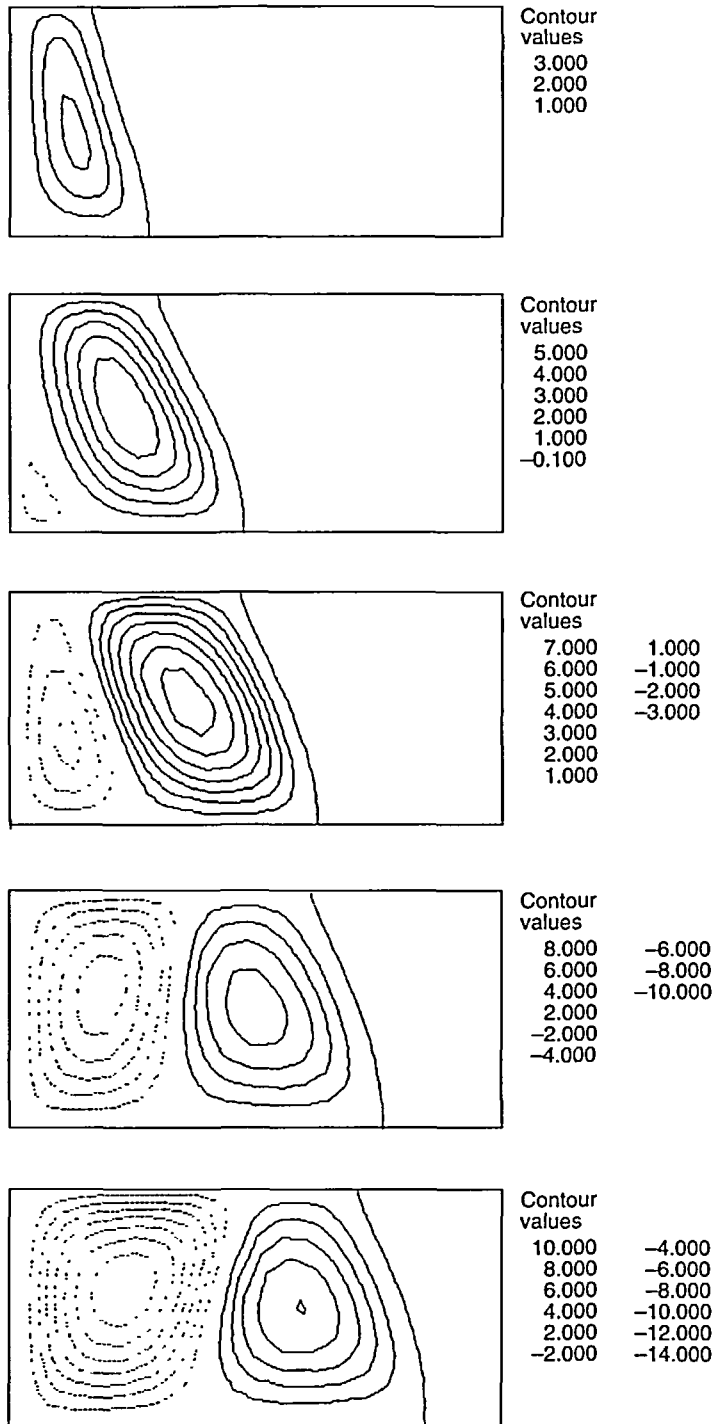


Figure 4 Streamline patterns in cavity with an aspect ratio of 0.5 for a modified Rayleigh Number of 10^6 for dimensionless hot wall temperatures of, from the top, 0.5, 0.6, 0.7, 0.8 and 0.85

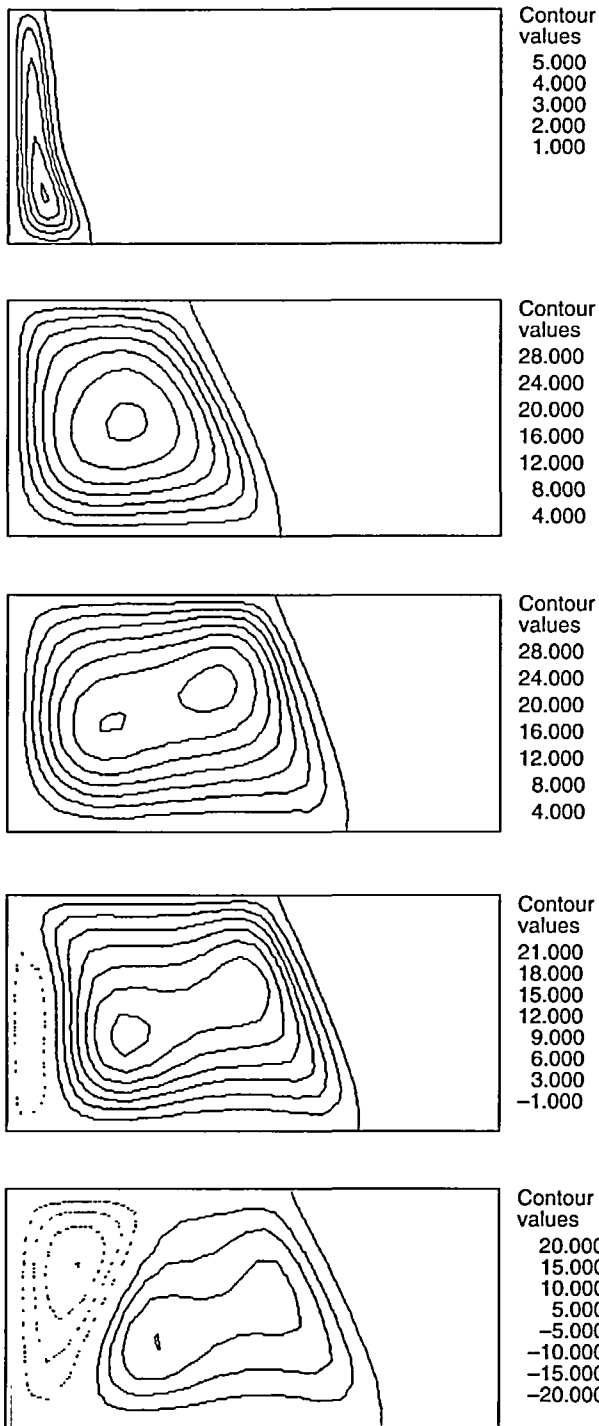


Figure 5 Streamline patterns in cavity with an aspect ratio of 0.5 for a modified Rayleigh Number of 10^7 for dimensionless hot wall temperatures of, from the top, 0.3, 0.4, 0.5, 0.6 and 0.65

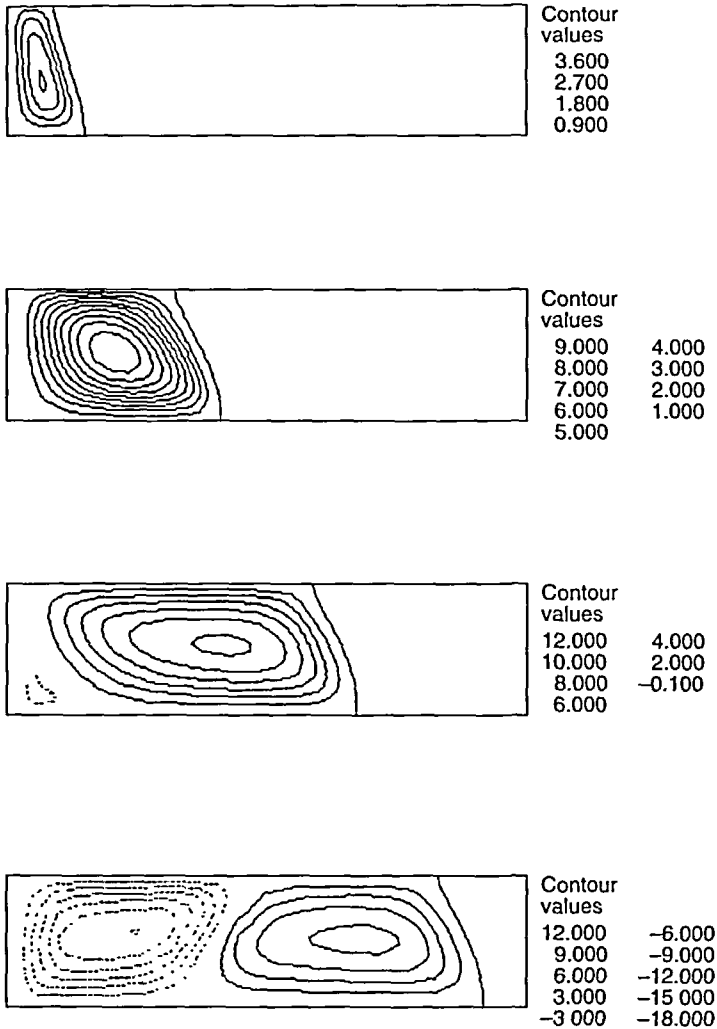


Figure 6 Streamline patterns in cavity with an aspect ratio of 0.25 for a modified Rayleigh Number of 10^7 for dimensionless hot wall temperatures of, from the top, 0.3, 0.4, 0.5 and 0.8

further increase in hot wall temperature, this opposite flow, which involves flow up the hot wall and down the cold wall, increases in intensity and becomes dominant bringing about a rise in Nusselt number with increasing hot wall temperature. The dimensionless wall temperature at which the convective motion starts to influence the Nusselt number increases with decreasing modified Rayleigh number, and at $Ra^* = 10^5$ the mean heat transfer rate remains essentially equal to the conduction up to the highest value of T_H considered. The effect of the governing parameters on the mean Nusselt number is further illustrated by the results given in Figure 10 which shows the variation of Nu with aspect ratio for various values of the dimensionless hot wall temperature for $Ra^* = 10^7$. It will be seen that the aspect ratio only starts to have a significant effect on the results when $A < 0.5$.

Attention will, lastly, be given to the mean dimensionless liquid layer thickness, Δ . Figures 11 and 12 show the variations of this dimensionless liquid layer thickness with dimensionless hot wall temperature for various values of the modified Rayleigh number for cavities with aspect

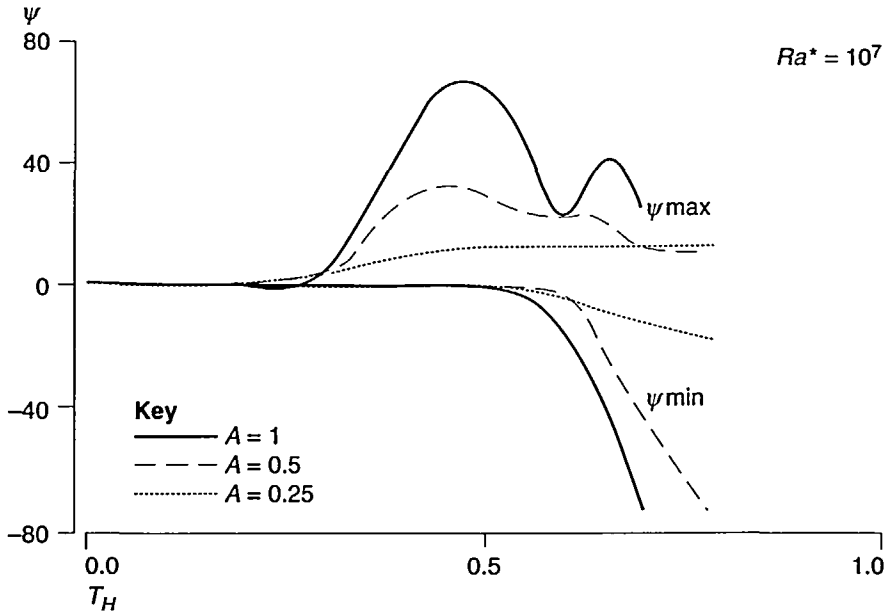


Figure 7 Variation of maximum and minimum values of the dimensionless stream function with dimensionless hot wall temperature for $Ra^* = 10^7$ for various cavity aspect ratios

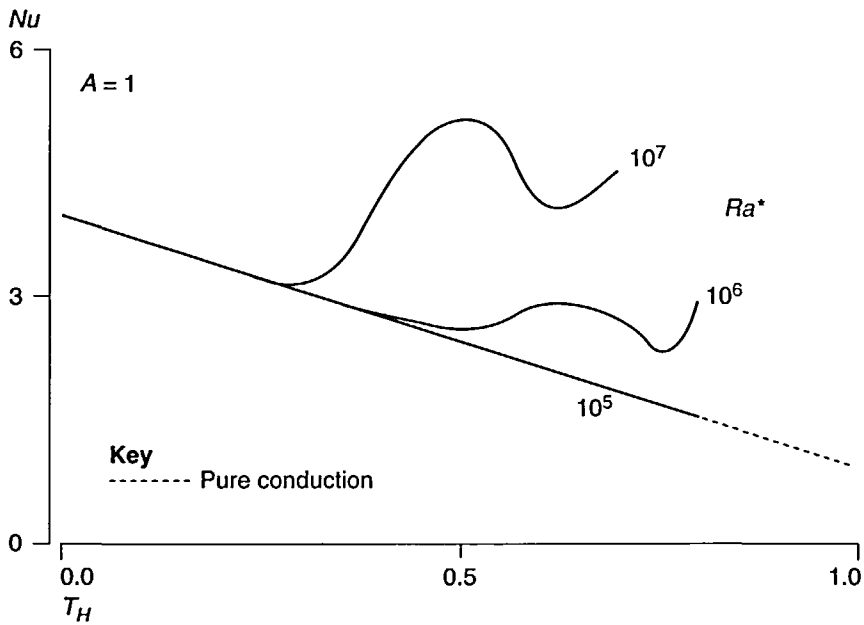


Figure 8 Variation of mean Nusselt number with dimensionless hot wall temperature for various modified Rayleigh numbers for a cavity with an aspect of ratio 1

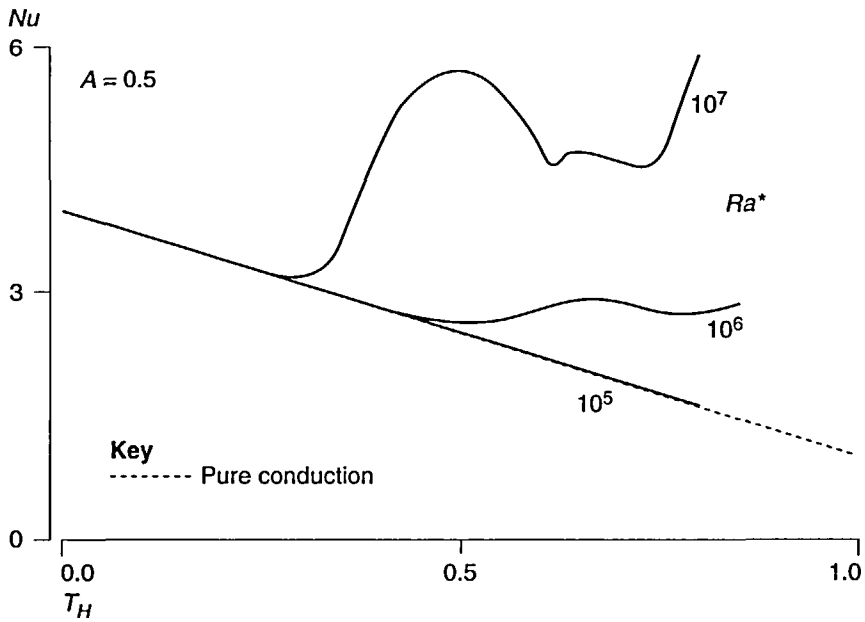


Figure 9 Variation of mean Nusselt number with dimensionless hot wall temperature for various modified Rayleigh Numbers for a cavity with an aspect ratio of 0.5

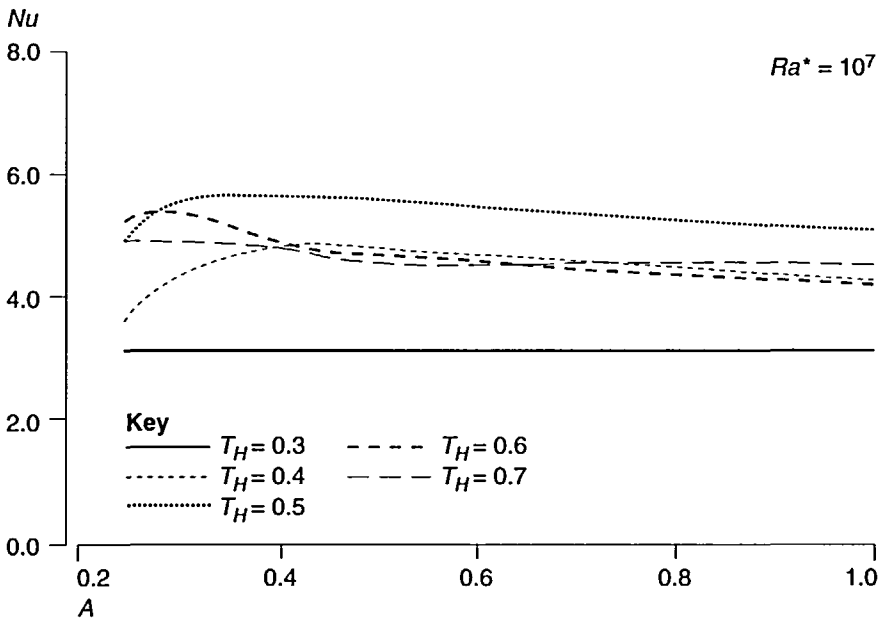


Figure 10 Variation of mean Nusselt number with cavity aspect ratio for $Ra^* = 10^7$ for various dimensionless hot wall temperatures, T_H

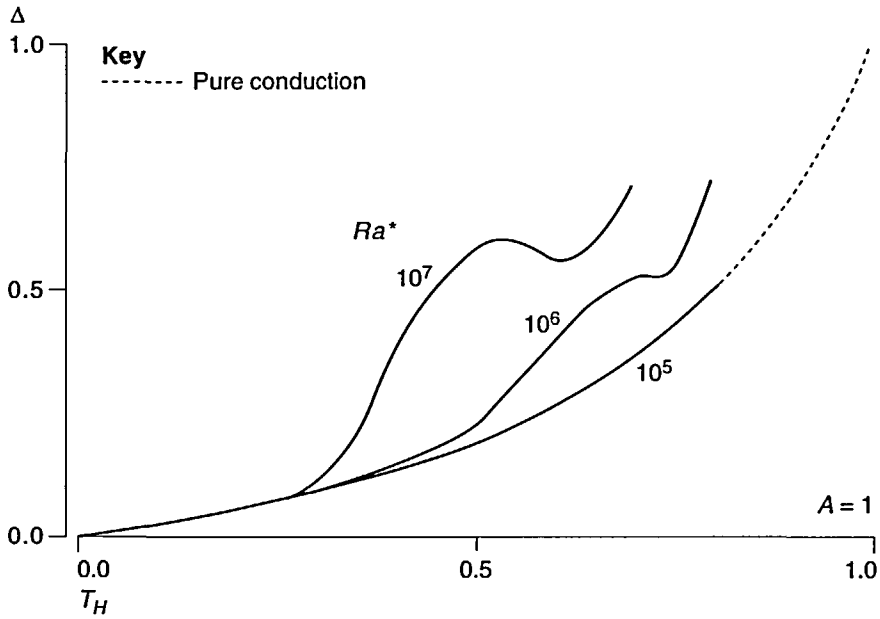


Figure 11 Variation of dimensionless liquid volume with dimensionless hot wall temperature for various modified Rayleigh numbers for a cavity with an aspect ratio of 1

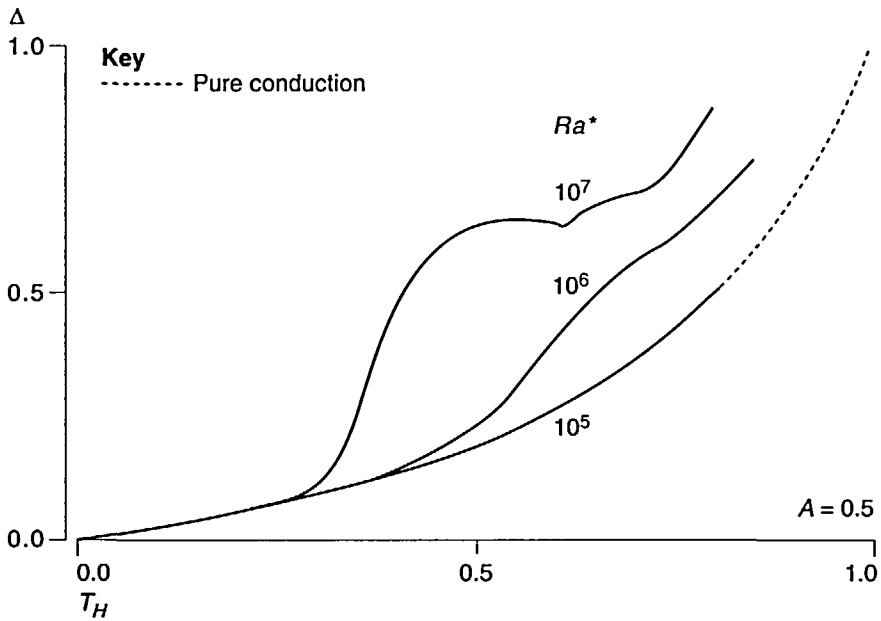


Figure 12 Variation of dimensionless liquid volume with dimensionless hot wall temperature for various modified Rayleigh numbers for a cavity with an aspect ratio of 0.5

ratios of 1 and 0.5 respectively. It will be seen from these figures that at low values of the dimensionless hot wall temperature the value of Δ is equal to the pure conduction value, the dimensionless thickness being given by:

$$\Delta = \frac{1}{1 + k_r(1 - T_H)/T_H}. \quad (12)$$

As the dimensionless wall temperature is increased, the values of Δ eventually start to rise above the conduction value at the higher modified Rayleigh number considered.

CONCLUSIONS

The results obtained in the present study indicate that:

- (1) At small values of the dimensionless wall temperature, the convective motion in the water has a negligible effect on the heat transfer rate and the mean Nusselt number and the dimensionless liquid volume under these conditions is given by the solution for pure conduction.
- (2) The value of the dimensionless wall temperature at which the convective motion starts to influence the flow decreases with increasing modified Rayleigh and, for the conditions covered in the present study, the convective motion had no influence for $Ra^* < 10^5$.
- (3) When the convective motion is important, the density inversion has a large effect on the motion in the water leading to a maximum and a minimum in the variation of mean Nusselt number with dimensionless wall temperature at a fixed modified Rayleigh number.
- (4) The aspect ratio of the cavity only begins to have a significant influence on the results when A is less than 0.5.

ACKNOWLEDGEMENT

This work was supported by the Natural Sciences and Engineering Research Council of Canada.

REFERENCES

- 1 Yao, L.S. and Prusa, J. Melting and freezing, *Advances in Heat Transfer*, **19**, 1-95 (1989)
- 2 Fukusako, S. and Yamada, M. Recent advances in research on freezing and melting heat-transfer phenomena, *Experimental Heat Transfer, Fluid Mechanics and Thermodynamics 1991*, J.F. Keffer, R.K. Shah and E.N. Ganic, eds, Elsevier, Barking, Essex and Amsterdam, 1157-1170 (1991)
- 3 Braga, S.L. and Viskanta, R. Effect of the water density extremum on the solidification process, *Experimental Heat Transfer, Fluid Mechanics and Thermodynamics 1991*, J.F. Keffer, R.K. Shah and E.N. Ganic, eds, Elsevier, Barking, Essex and Amsterdam, 1185-1192 (1991)
- 4 de Vahl Davis, G., Leonardi, E., Wong, P.H. and Yeoh, G.H. Natural convection in a solidifying liquid, *Numerical Methods in Thermal Problems*, R.W. Lewis and K. Morgan, eds, Pineridge Press, Swansea, **6**, (1) 410-420 (1989)
- 5 Oosthuizen, P.H. Numerical study of the steady state freezing of water in a rectangular enclosure, *Numerical Methods in Thermal Problems*, R.W. Lewis, ed., Pineridge Press, Swansea, **VIII**, (1), 92-103 (1993)
- 6 Inaba, H. and Fukada, T. Natural convection in an inclined square cavity in regions of density inversion of water, *Journal of Fluid Mechanics*, **142**, 363-381 (1984)
- 7 Lankford, K.E. and Bejan, A. Natural convection in a vertical enclosure filled with water near 4°C, *Journal of Heat Transfer*, **108**, 755-763 (1986)
- 8 Ivey, G.N. and Hamblin, P.F. Convection near the temperature of maximum density for high Rayleigh number, low aspect ratio, rectangular cavities, *Journal of Heat Transfer*, **111**, 100-104 (1989)
- 9 Oosthuizen, P.H. and Paul, J.T. Unsteady free convective flow in an enclosure containing water near its maximum density, *Proc. 1990 AIAA/ASME Thermophysics and Heat Transfer Conference ASME HTD-140*, 83-91 (1990)